International Journal of Solids and Structures 47 (2010) 3254–3262

Contents lists available at ScienceDirect

International Journal of Solids and Structures

journal homepage: www.elsevier.com/locate/ijsolstr

Resonant behavior of a membrane of a dielectric elastomer

Jian Zhu, Shengqiang Cai, Zhigang Suo *

School of Engineering and Applied Sciences, Harvard University, Cambridge, MA 02138, United States

ARTICLE INFO

Article history:
Received 20 May 2010
Received in revised form 18 July 2010
Available online 13 August 2010

Keywords:
Dielectric elastomer actuator
Large deformation
Nonlinear dynamics
Membrane

ABSTRACT

This paper analyzes a membrane of a dielectric elastomer, prestretched and mounted on a rigid circular ring, and then inflated by a combination of pressure and voltage. Equations of motion are derived from a nonlinear field theory, and used to analyze several experimental conditions. When the pressure and voltage are static, the membrane may attain a state of equilibrium, around which the membrane can oscillate. The natural frequencies can be tuned by varying the prestretch, pressure, or voltage. A sinusoidal pressure or voltage may excite superharmonic, harmonic, and subharmonic resonance. Several modes of oscillation predicted by the model have not been reported experimentally, possibly because these modes have small deflections, despite large stretches.

1. Introduction

Dielectric elastomers are being developed intensely as electromechanical transducers (e.g., Pelrine et al., 2000; Carpi et al., 2008). Most studies have focused on the quasi-static behavior of large deformation for applications such as soft robots, adaptive optics, energy harvesting, and programmable haptic surfaces (Carpi et al., 2008). It has been appreciated, however, that dielectric elastomers can deform over a wide range of frequencies. Applications exploiting the dynamic behavior of dielectric elastomers include loudspeakers (Heydt et al., 2006; Chiba et al., 2007), active noise control (Heydt et al., 2000), and frequency tuning (Dubois et al., 2008). Furthermore, inertia can play a significant role whenever devices operate at high frequencies. For example, when an elastomeric pump is driven rapidly, the membrane can resonate with the excitation (Goulbourne et al., 2007).

This paper focuses on the dynamic behavior of dielectric elastomers. While dynamics of membranes is a classical topic (e.g., Farlow, 1993; Goncalves et al., 2009), few theoretical analyses have been devoted to dielectric elastomers. Mockensturm and Goulbourne (2006) investigated a time response of a spherical membrane for a specified applied voltage. Dubois et al. (2008) demonstrated that the frequency of a flat membrane can be tuned by a voltage. Zhu et al. (2010) studied nonlinear oscillation of a spherical membrane, and showed that the membrane exhibits subharmonic and superharmonic resonance, as well as harmonic resonance.

This paper goes beyond spherical and flat membranes, and analyzes a prestretched membrane mounted on a rigid ring, inflated by a pressure and a voltage into an axisymmetric shape, Fig. 1. This configuration has been used in experiments by several groups (Ha et al., 2006; Heydt et al., 2006; Goulbourne et al., 2007; Fox and Goulbourne, 2008, 2009). When a membrane undergoes deformation of the spherical symmetry, the field is homogeneous, governed by an ordinary differential equation. By contrast, when a membrane undergoes deformation of the axisymmetric symmetry as shown in Fig. 1, the field is inhomogeneous (in the longitudinal direction), governed by partial differential equations. The inhomogeneous deformation enables the membrane to resonate at multiple frequencies of excitation, as observed in recent experiments (Fox, 2007; Fox and Goulbourne, 2008, 2009). Furthermore, it is interesting to explore subharmonic and superharmonic resonance besides harmonic resonance when the deformation is inhomogeneous.

This paper is planned as follows. Section 2 derives the equations of motion for an axisymmetric membrane, subject to a pressure and a voltage, undergoing dynamic and finite deformation. Section 3 analyzes stability of states of equilibrium when the pressure and voltage are static. For a given prestretch, a membrane can attain a stable state of equilibrium when the pressure and voltage stay below certain critical conditions. Section 4 studies a membrane oscillating around a state of equilibrium, and shows that the natural frequencies can be tuned by changing the prestretch, pressure, or voltage. Section 5 shows that sinusoidal pressure or voltage can excite superharmonic, harmonic, and subharmonic responses. Section 6 compares the theoretical results with available experimental observations.

2. Equations of motion

This section derives the equations of motion for an axisymmetric membrane of a dielectric elastomer subject to a pressure and a voltage. Similar equations of motion have been derived on the

* Corresponding author. Tel.: +1 617 4953789; fax: +1 617 4960601.
E-mail address: suo@seas.harvard.edu (Z. Suo).

0020-7683/$ - see front matter © 2010 Elsevier Ltd. All rights reserved.
doi:10.1016/j.ijsolstr.2010.08.008

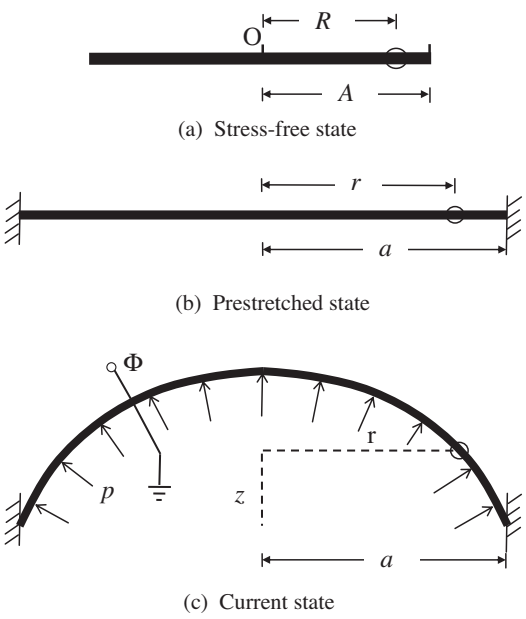

Fig. 1. Cross section of a membrane of a dielectric elastomer, sandwiched between two compliant electrodes. (a) In the stress-free state, the elastomer is a circular flat membrane. (b) The membrane is prestretched and held by a rigid ring. (c) Subject to a pressure and a voltage, the membrane inflates out of the plane, and takes an axisymmetric shape.

basis of the Maxwell stress (e.g., Fox and Goulbourne, 2009). Here we derive the equations of motion in an approach such that the equations can be readily modified even if the Maxwell stress is not valid (Suo et al., 2008).

Fig. 1 illustrates the cross section of a membrane of a dielectric elastomer, sandwiched between two compliant electrodes. In the absence of any applied load, the membrane is of a circular shape, thickness H and radius A. This state is taken to be the state of reference, in which we mark a material particle by its distance R from the center O. When the membrane is prestretched and attached to a rigid circular ring of radius a, the particle R moves to the place a distance r from the center. The membrane is then inflated by a time-dependent pressure $p(t)$ and a voltage $\Phi(t)$. At time t, the membrane is assumed to deform into an axisymmetric shape, and the particle R moves to a place with coordinates r and z. The two fields, $r(R,t)$ and $z(R,t)$, specify the time-dependent deformation of the membrane.

Consider a differential element between two particles R and $R + dR$. At time t, one particle occupies the place of coordinates $r(R,t)$ and $z(R,t)$, and the other particle occupies the place of coordinates $r(R + dR,t)$ and $z(R + dR,t)$. Let $l(R,t)$ be the arclength between the element and the center of the membrane, and $\theta(R,t)$ be the slope of the element. Consequently, $r(R + dR,t) - r(R,t) = \cos\theta dl$ and $z(R + dR,t) - z(R,t) = -\sin\theta dl$. The longitudinal stretch is defined by the length of the element at time t divided by the length of the element in the state of reference, $\lambda_1 = \partial l/\partial R$, namely,

$$\lambda_1 = \sqrt{\left(\frac{\partial r}{\partial R}\right)^2 + \left(\frac{\partial z}{\partial R}\right)^2}. \tag{1}$$

Next consider the circle of material particles, of perimeter $2\pi R$ in the state of reference. At time t, the circle is of perimeter $2\pi r$. The latitudinal stretch is

$$\lambda_2 = \frac{r}{R}. \tag{2}$$

The volume enclosed by the membrane is given by

$$v = -\int \pi r^2 \frac{\partial z}{\partial R} dR. \tag{3}$$

All integrals in this paper are taken with respect to R over the interval $(0,A)$.

Define the nominal electric displacement $\widetilde{D}(R,t)$ by the electric charge on an element of an electrode at time t divided by the area of the element in the state of reference. Consequently, the total charge on the electrode is

$$Q = 2\pi \int \widetilde{D} R dR. \tag{4}$$

The actuator is a thermodynamic system, taken to be held at a constant temperature. Let W be the Helmholtz free energy of an element of the dielectric at time t divided by the volume of the element in the state of reference. The elastomer is taken to be incompressible, so that the thermodynamic state of an element of the membrane is described by two stretches, λ_1 and λ_2, as well as the nominal electric displacement $\widetilde{D}$. A material model of the membrane is specified by a free-energy function

$$W = W\left(\lambda_1, \lambda_2, \widetilde{D}\right). \tag{5}$$

For small variations in the kinematic variables, the free-energy density varies by

$$\delta W = s_1 \delta\lambda_1 + s_2 \delta\lambda_2 + \widetilde{E}\delta\widetilde{D}, \tag{6}$$

where s_1 and s_2 are the nominal stresses, and $\widetilde{E}$ is the nominal electric field. Eq. (6) relates these nominal quantities to partial differential coefficients of the free-energy function:

$$s_1 = \frac{\partial W\left(\lambda_1, \lambda_2, \widetilde{D}\right)}{\partial \lambda_1}, \tag{7}$$

$$s_2 = \frac{\partial W\left(\lambda_1, \lambda_2, \widetilde{D}\right)}{\partial \lambda_2}, \tag{8}$$

$$\widetilde{E} = \frac{\partial W\left(\lambda_1, \lambda_2, \widetilde{D}\right)}{\partial \widetilde{D}}. \tag{9}$$

Once a free-energy function $W\left(\lambda_1, \lambda_2, \widetilde{D}\right)$ is prescribed for a material, (7)–(9) constitute the equations of state.

For an arbitrary variation of the system, the change in the Helmholtz free energy of the membrane equals the work done by the pressure, voltage, and inertial forces, namely,

$$2\pi H \int \delta W R dR = p\delta v + \Phi\delta Q - 2\pi H\rho \int \left(\frac{\partial^2 r}{\partial t^2}\delta r + \frac{\partial^2 z}{\partial t^2}\delta z\right) R dR, \tag{10}$$

where ρ is the mass density of the elastomer. Regarding δr, δz and $\delta\widetilde{D}$ as independent variations, we obtain from the standard calculus of variation that

$$-\frac{\partial}{R\partial R}(Rs_1 \sin\theta) + \lambda_1\lambda_2 \frac{p}{H}\cos\theta = \rho\frac{\partial^2 z}{\partial t^2}, \tag{11}$$

$$\frac{\partial}{R\partial R}(Rs_1 \cos\theta) - \frac{s_2}{R} + \lambda_1\lambda_2 \frac{p}{H}\sin\theta = \rho\frac{\partial^2 r}{\partial t^2}, \tag{12}$$

$$H\widetilde{E} = \Phi. \tag{13}$$

The equations of motion, (11) and (12), can also be obtained by considering the membrane between R and $R + dR$, and balancing forces at time t in the directions of z and r, respectively. Eq. (13) recovers the definition of the nominal electric field.

The above equations are valid for an arbitrary material model specified by the free-energy function, $W\left(\lambda_1, \lambda_2, \widetilde{D}\right)$. In what follows, we adopt a material model known as the ideal dielectric elastomer (Zhao et al., 2007), where the dielectric behavior of the

elastomer is taken to be liquid-like, unaffected by deformation. Specifically, the true electric displacement is linear in the true electric field, and the permittivity is independent of deformation. This material model seems to describe some experimental data (Kofod et al., 2003), but is inconsistent with other experimental data (Wissler and Mazza, 2007). Nevertheless, this model has been used almost exclusively in previous analyses of dielectric elastomers. See Zhao and Suo (2008a) for a model of nonideal dielectric elastomers, and Bustamante et al. (2009) for a more general description of electromechanical interaction.

The elastomer is assumed to be incompressible, so that the stretch in the thickness direction of the membrane, λ_3, relates to the stretches in the surface of the membrane as $\lambda_3 = 1/(\lambda_1\lambda_2)$. The thickness of the membrane is H in the undeformed state, and is $\lambda_3 H = H/(\lambda_1\lambda_2)$ in the deformed state. By definition, the true electric field E is the voltage divided by the thickness of the membrane in the deformed state, so that $E = \lambda_1\lambda_2\Phi/H = \lambda_1\lambda_2\widetilde{E}$. The true electric displacement D is defined as the charge in the deformed state divided by the area of the membrane in the deformed state, so that $D = \widetilde{D}/(\lambda_1\lambda_2)$.

For the ideal dielectric elastomer, following Zhao et al. (2007), we assume that the Helmholtz free energy takes the form

$$W\left(\lambda_1, \lambda_2, \widetilde{D}\right) = \frac{\mu}{2}\left(\lambda_1^2 + \lambda_2^2 + \lambda_1^{-2}\lambda_2^{-2} - 3\right) + \frac{\widetilde{D}^2}{2\varepsilon}\lambda_1^{-2}\lambda_2^{-2}. \tag{14}$$

The first term is the elastic energy, where μ is the small strain shear modulus. The second term is the dielectric energy, where ε is the permittivity. The elastomer is taken to be a network of long polymers obeying the Gaussian statistics, so that the elastic behavior of the elastomer is neo-Hookean. For an ideal dielectric elastomer, the dielectric energy per unit volume is $D^2/2\varepsilon$, and the permittivity ε is a constant independent of deformation. In (14) the dielectric energy has been expressed in terms of the nominal electric displacement $\widetilde{D}$, a variable required by the function $W\left(\lambda_1, \lambda_2, \widetilde{D}\right)$.

Inserting (14) into (7)–(9), we obtain the equations of state:

$$s_1 = \mu\left(\lambda_1 - \lambda_1^{-3}\lambda_2^{-2}\right) - \frac{\widetilde{D}^2}{\varepsilon}\lambda_1^{-3}\lambda_2^{-2}, \tag{15}$$

$$s_2 = \mu\left(\lambda_2 - \lambda_2^{-3}\lambda_1^{-2}\right) - \frac{\widetilde{D}^2}{\varepsilon}\lambda_2^{-3}\lambda_1^{-2}, \tag{16}$$

$$\widetilde{E} = \frac{\widetilde{D}}{\varepsilon}\lambda_1^{-2}\lambda_2^{-2}. \tag{17}$$

Recall that the true stresses σ_1 and σ_2 relate to the nominal stresses as $\sigma_1 = \lambda_1 s_1$ and $\sigma_2 = \lambda_2 s_2$. We rewrite (15)–(17) in terms of the true quantities:

$$\sigma_1 = \mu\left(\lambda_1^2 - \lambda_1^{-2}\lambda_2^{-2}\right) - \varepsilon E^2, \tag{18}$$

$$\sigma_2 = \mu\left(\lambda_2^2 - \lambda_2^{-2}\lambda_1^{-2}\right) - \varepsilon E^2, \tag{19}$$

$$D = \varepsilon E. \tag{20}$$

These equations are readily interpreted. For example, the first term in (18) is the contribution to the stress due to the change of entropy associated with the stretch of the polymer network, and the second term is due to the applied voltage. Eqs. (18)–(20) in various forms has been used in previous analyses (e.g., Pelrine et al., 2000; Wissler and Mazza, 2005; Goulbourne et al., 2005).

3. State of equilibrium and critical condition

When the pressure p and voltage Φ are static, the membrane may reach a state of equilibrium. The state of equilibrium is described by time-independent functions $r_0(R)$ and $z_0(R)$, governed by the equations in Section 2, setting $\partial^2 z/\partial t^2 = 0$ and $\partial^2 r/\partial t^2 = 0$. We solve these equations by using MATLAB. We normalize the coordinates by A, the pressure by $(H\mu/A)$, and the voltage by $\left(H\sqrt{\mu/\varepsilon}\right)$. Unless otherwise stated, we fix the prestretch $\lambda_0 = a/A = 3$.

Fig. 2 plots the deformed shapes of the membrane subject to various pressures and voltages. As expected, the displacement of the membrane increases with the pressure and voltage. Our simulation shows (e.g., Fig. 2a) that the shape of the membrane differs from a spherical cap, especially when the voltage is large.

Fig. 3 plots the distribution of the stretches λ_1 and λ_2 when the membrane is subject to a fixed pressure and several values of voltage. The deformation of the membrane is inhomogeneous. At a fixed pressure and voltage, both λ_1 and λ_2 are largest at the center of the membrane, and monotonically reduces to the smallest value at the outer end. As a result, the center point of the membrane is the weakest point for mechanical failure. At the ring, the latitudinal stretch remains fixed by the pre-stretch, $\lambda_2(A) = \lambda_0$.

Fig. 4 plots the pressure as a function of the volume, when the membrane is subject to a constant voltage. As the membrane inflates, the pressure first increases, reaches a peak, and then decreases. The peak pressure corresponds to a critical state. When the applied pressure is above the peak, the membrane cannot reach a state of equilibrium. When the applied pressure is below the peak, corresponding to each value of pressure are two values of volume. The value of volume on the rising part of the pressure-volume curve corresponds to a stable state, while the value of volume on the descending part corresponds to an unstable state. Also plotted in Fig. 4 is the fundamental natural frequency as a function of the volume. When the pressure reaches the peak, the fundamental natural frequency vanishes. The method to calculate natural frequencies is described in the next section.

When the pressure and voltage are small, the system will oscillate around a stable state of equilibrium. When the pressure or voltage reaches a critical value at the peak, the natural frequency vanishes, and it takes an infinite time for the system to return to the state of equilibrium. In other words, the state of equilibrium becomes unstable. Indeed, for many mechanical systems a vanishing natural frequency indicates instability or buckling (Zhu et al., 2008; Hwang and Perkins, 1994).

Fig. 5 plots the critical values of p and Φ at several levels of prestretch λ_0. At a fixed prestretch λ_0, when the pressure and voltage

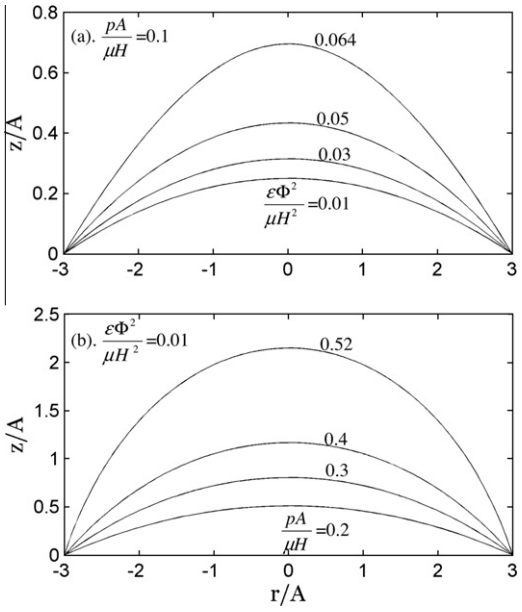

Fig. 2. Deformed shapes of the membrane subject to (a) a fixed pressure and several values of voltage, and (b) a fixed voltage and several values of pressure.

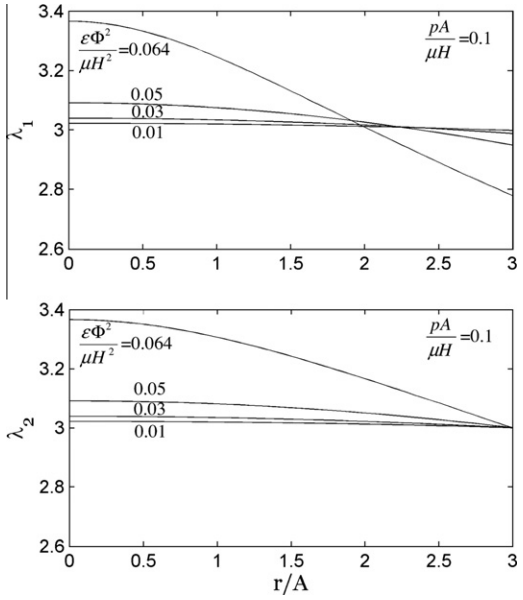

Fig. 3. The distributions of the longitudinal stretch and the latitudinal stretch in the membrane subject to a fixed pressure and several values of voltage.

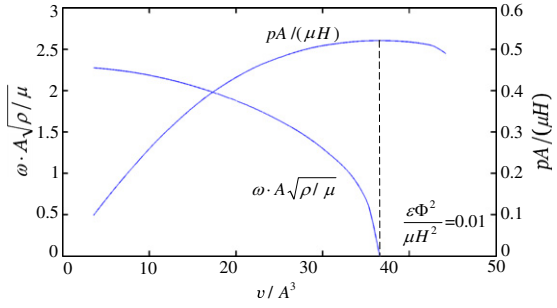

Fig. 4. The pressure and the fundamental frequency are plotted as functions of the volume enclosed by the membrane. When the pressure reaches the peak, the fundamental frequency vanishes.

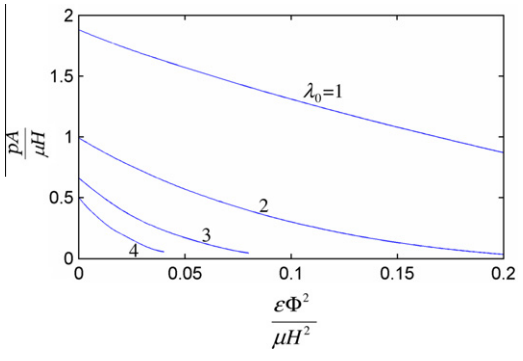

Fig. 5. Plotted on the plane of (p, Φ) are curves of the critical values at several levels of prestretch λ_0. At a fixed λ_0, each point on the corresponding curve represents a critical state of the membrane. When the pressure and voltage fall above this curve, the membrane cannot reach a state of equilibrium. When the pressure and voltage fall below the curve, the membrane can reach a stable state of equilibrium.

fall above the corresponding curve, the membrane cannot reach a state of equilibrium. However, when the pressure and voltage fall below the curve, the membrane can reach a state of equilibrium. For the membranes with the same original radius and thickness A and H, as indicated in Fig. 5, the critical values of p and Φ for instability decrease with the prestretch. When the prestretch is fixed, the critical value of p (or Φ) decreases with Φ (or p).

For a neo-Hookean material, when the pressure or voltage reaches the peak, we assume that the deformation of the membrane may go to infinity, which leads to electrical breakdown. However, elastomers used in practice may exhibit strain-stiffening due to the finite contour length of polymer chains. This phenomenon cannot be described by a neo-Hookean model, but can be described by other stress-strain models (e.g., Arruda and Boyce, 1993). For an Arruda–Boyce material, when the pressure or voltage reaches a critical value, the membrane may undergo snap-through instability and jump to a state of equilibrium at a larger stretch. In this paper, we focus on electromechanical instability of a membrane of a dielectric elastomer. For example, Fig. 5 shows the effect of the prestretch on the critical state for electromechanical instability. However, for dielectric elastomers, how to survive snap-through instability and achieve a larger deformation of actuation is an interesting and important issue and deserves further studies (Suo and Zhu, 2009; Zhao and Suo, 2010).

4. Oscillation around a state of equilibrium

As discussed in the previous section, a membrane subject to a constant pressure and voltage may reach a state of equilibrium. Around the state of equilibrium, the membrane can oscillate. We now analyze oscillation of small amplitude. When the membrane oscillates around the state of equilibrium, $r_0(R)$ and $z_0(R)$, we write a mode of oscillation as:

$$r(R,t) = r_0(R) + \hat{r}(R)\sin\omega t, \tag{21}$$

$$z(R,t) = z_0(R) + \hat{z}(R)\sin\omega t. \tag{22}$$

Thus, the mode of oscillation has the natural frequency ω, and has the field of amplitude $\hat{r}(R)$ and $\hat{z}(R)$. Using the finite difference method, we divide the domain [0,A] into N elements (say, $N = 1000$). Substituting (21) and (22) into (11) and (12), we obtain the equations for each element and then expand them into the power series of $\hat{r}$ and $\hat{z}$. The resulting equations are lengthy and are not listed here. For oscillation of small amplitude, we retain terms linear in $\hat{r}$ and $\hat{z}$, and assemble the equations of the entire system as:

$$Kx = \omega^2 x \tag{23}$$

where $x \quad (= [\hat{r}(0)\hat{z}(0)\hat{r}(A/N)\hat{z}(A/N)\ldots\hat{r}(A-A/N)\hat{z}(A-A/N)\hat{r}(A)\hat{z}(A)]^{\mathrm{T}})$ is the amplitude vector, and K is a stiffness matrix with each element K_{ij} dependent on the state of equilibrium $r_0(R)$ and $z_0(R)$. The procedure leads to an eigenvalue problem, with ω^2 being the eigenvalue, and x being the eigenfunction. The lengths of the eigenfunctions are normalized by A, such that $|x/A| = 1$), and the frequencies are normalized by $A^{-1}\sqrt{\mu/\rho}$.

When $\frac{pA}{\mu H} = 0.1$ and $\frac{\varepsilon\Phi^2}{\mu H^2} = 0.01$, the normalized natural frequencies of the first seven modes are $\omega_1 = 2.3$, $\omega_2 = 3.7$, $\omega_3 = 5.2$, $\omega_4 = 6.7$, $\omega_5 = 8.2$, $\omega_6 = 9.7$, and $\omega_7 = 11.2$. Fig. 6 plots the shape and the longitudinal and latitudinal stretches of the 1st, 3rd, 5th, and 7th modes, while Fig. 7 plots those of the 2nd, 4th, and 6th modes. For the even modes, the shapes of different modes are nearly indistinguishable (Fig. 7a), but the stretches of different modes are quite different (Fig. 7b, c). The significance of these modes will be discussed in Section 6 in connection to parametric excitation.

5. Tuning natural frequencies

Many devices require that natural frequencies be tuned. Examples include MEMS-based oscillators used in sensing (Ekinci et al., 2004), timing, and frequency reference (Nguyen, 2007). As another

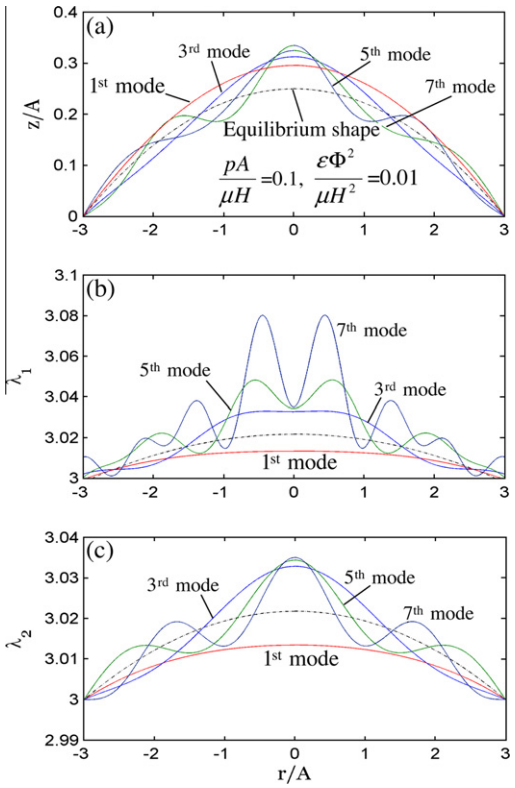

Fig. 6. The 1st, 3rd, 5th, and 7th modes of oscillation around a state of equilibrium (indicated by dashed lines), (a) Shape of the membrane, (b) Longitudinal stretch, (c) Latitudinal stretch.

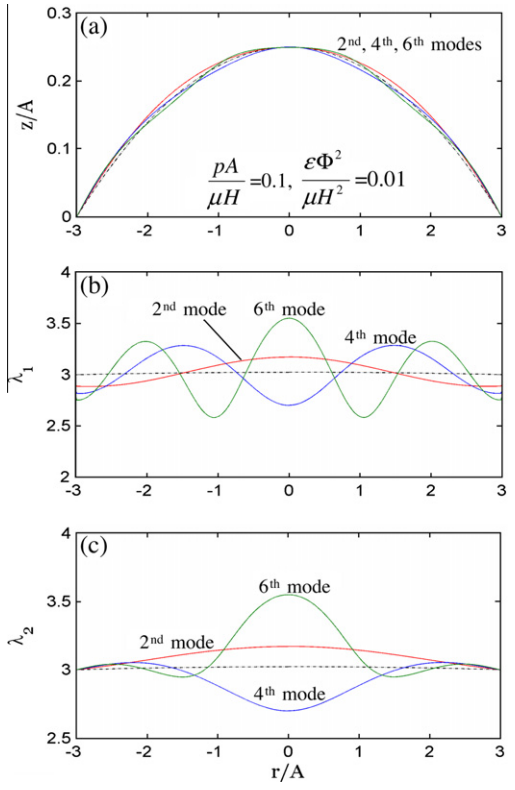

Fig. 7. The 2nd, 4th and 6th modes of oscillation around a state of equilibrium (indicated by dashed lines), (a) Shape of the membrane, (b) Longitudinal stretch, (c) Latitudinal stretch.

example, the natural frequency of an energy harvester is often tuned into the spectrum where most of the energy is available (Anton and Sodano, 2007). For many systems, however, natural frequencies are set by materials and geometries, and are often difficult to tune (Cottone et al., 2009). By contrast, the natural frequency of a dielectric elastomer is easily varied by varying the prestretch during fabrication, and by varying the pressure or voltage during operation (Dubois et al., 2008).

Fig. 8 plots the fundamental frequency as a function of the prestretch, while the pressure and voltage are held at several constant levels. It is well known that, in the absence of pressure and voltage, the frequency of a membrane increases with the prestretch (Den Hartog, 1985). By contrast, when the membrane is subject to a constant pressure and voltage, as the prestretch increases, the frequency first increases, reaches a peak, and then decreases. This trend is understood as follows. When the prestretch is small, the stress in the membrane increases with prestretch, and the frequency increases. For a given prestretch, the membrane reaches the critical state at certain levels of pressure and voltage (Fig. 5), and the frequency becomes zero.

Fig. 9 plots the fundamental frequency as a function of the pressure at several levels of voltage. When the prestretch is small ($\lambda_0 = 1.1$), as the pressure increases, the fundamental frequency first increases, reaches a peak, and then decreases. When the prestretch is large ($\lambda_0 = 3$), the fundamental frequency decreases as the pressure increases.

6. Parametric excitation

When the pressure or the voltage varies with time, the behavior of the membrane can be very complex. To illustrate the complexity, we prescribe a static pressure p and a sinusoidal voltage:

$$\Phi(t) = \Phi_{dc} + \Phi_{ac} \sin \Omega t, \tag{24}$$

where Φ_{dc} is the dc voltage, Φ_{ac} the amplitude of ac voltage, and Ω the frequency of excitation. As shown in Section 2, the AC voltage appears as a time-varying coefficient in the partial differential equations. Phenomena of this type are known as parametric excitation (Jordan and Smith, 1987; Nayfeh and Mook, 1979).

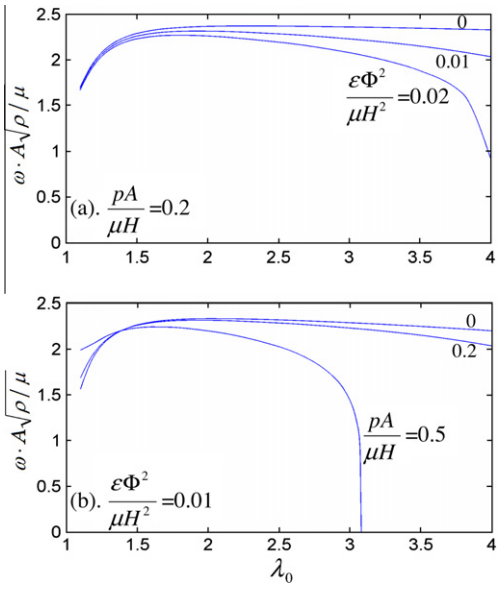

Fig. 8. The fundamental frequency is plotted as a function of the prestretch, (a) when the membrane is subject to a fixed pressure and several values of voltage, or (b) when the membrane is subject to a fixed voltage and several values of pressure.

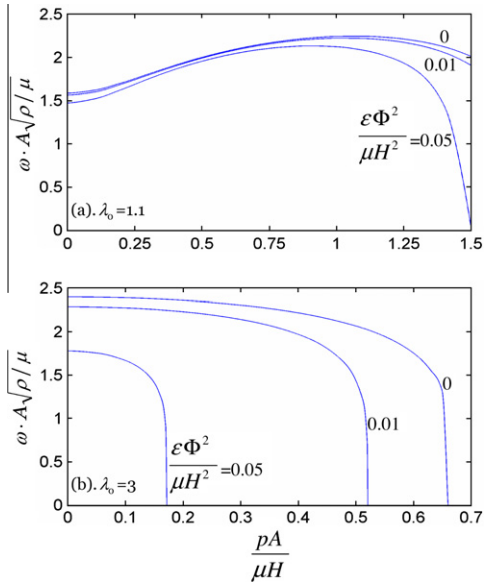

Fig. 9. The fundamental frequency is plotted as a function of the pressure at several values of voltage, (a) $\lambda_0 = 1.1$, (b) $\lambda_0 = 3$.

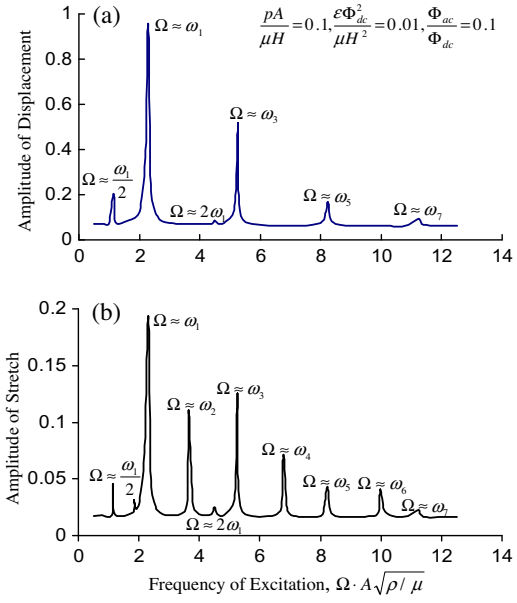

Fig. 10. Under a static pressure and a sinusoidal voltage, a membrane resonates at several frequencies of excitation, which are closely related to natural frequencies of various modes, (a) The amplitude of displacement as a function of the frequency of excitation, (b) The amplitude of stretch as a function of the frequency of excitation.

The nonlinear theory described in Section 2 has been embedded in the finite element software ABAQUS with a user-supplied subroutine (Zhao and Suo, 2008b). We use this code to simulate the following process. First, the membrane is uniformly prestretched in the radial direction, and then fixed along the edge. Second, the membrane is subject to a static pressure. Finally, a sinusoidal voltage is applied, which causes the membrane to oscillate. Fig. 10 plots the amplitudes of displacement and stretch, at the center of the membrane, as functions of the frequency of excitation. Here the amplitude is defined as the difference between the highest and lowest values of displacement or stretch. As we know, the actuation for a dielectric elastomer is related to Φ^2. When the voltage is sinusoidal (24), note that

$$\Phi^2 = \Phi_{dc}^2 + 2\Phi_{dc}\Phi_{ac}\sin\Omega t + \Phi_{ac}^2\sin^2\Omega t. \tag{25}$$

The ac voltage with the frequency Ω leads to the excitations with two different frequencies, namely, $2\Phi_{dc}\Phi_{ac}\sin(\Omega t)$ and $0.5\Phi_{ac}^2\cos(2\Omega t)$. In this numerical example, we have set $\Phi_{ac}/\Phi_{dc} = 0.1$, so that the excitation of the frequency of 2Ω may be neglected in the discussion.

When the frequency of excitation is close to one of the natural frequencies, the corresponding natural vibration mode is induced. The even modes have small amplitude of displacement, but large amplitude of stretch. Thus, we may think the even modes are related to in-plane vibration, while the odd modes are related to out-of-plane vibration. The existing literature on dynamic behavior of membrane focused on out-of-plane oscillation, but did not report in-plane oscillation (e.g., Goncalves et al., 2009; Fox, 2007; Fox and Goulbourne, 2008, 2009). The shapes of the out-of-plane modes reported in the literature are similar to our results shown in Fig. 6.

Besides the harmonic resonance, our analysis shows that the membrane also resonates when $\Omega \approx 2\omega_1$, which is known as subharmonic resonance (Nayfeh and Mook, 1979). In addition, the membrane resonates when $\Omega \approx \omega_1/2$, which is known as superharmonic resonance. Fig. 11 plots the displacement at the center of the membrane as a function of time. The membrane is driven at several frequencies of excitation. When $\Omega \approx \omega_1$, the membrane oscillates at a frequency close to the frequency of excitation, indicative of the harmonic resonance of the fundamental mode. When $\Omega \approx \omega_3$, the membrane oscillates at a frequency close to the frequency of excitation, indicative of the harmonic response of the third mode. When $\Omega \approx \omega_1/2$, the membrane oscillates at the frequency ω_1, which doubles the frequency of excitation, indicative of superharmonic resonance. When $\Omega \approx 2\omega_1$, the membrane oscillates at the frequency ω_1, which is half of the frequency of excitation, indicative of subharmonic resonance. Subharmonic and superharmonic responses are common phenomena in nonlinear oscillations due to parametric excitation (Turner et al., 1998; De and Aluru, 2005).

When designing a loudspeaker of a dielectric elastomer (Heydt et al., 2006; Chiba et al., 2007), one wishes that the frequency of output vibration is the same as that of input signal. Fig. 11 shows that in some ranges of frequency, for example, when Ω is close to $\omega_1/2$ or $2\omega_1$, the membrane oscillates at a frequency different from the frequency of excitation. This phenomenon will distort sound. To avoid this distortion, one should tune the natural frequency of a dielectric elastomer far away from half and double the frequency of excitation.

7. Comparison with experimental observations

Recently, Fox and Goulbourne studied dynamics of dielectric elastomer membranes experimentally (Fox, 2007; Fox and Goulbourne, 2008, 2009). The membrane VHB 4905 or VHB 4910 with a diameter of 3.5″ is prestretched mechanically first (with $\lambda_0 = 3$), and then fixed by a rigid frame (Fox and Goulbourne, 2008). Carbon grease, spread on both sides of the membrane, serves as the electrodes. The membrane deforms under a pressure and a voltage. Fox measured the dynamic responses of the membrane due to i) a time-varying pressure and a fixed DC voltage, and ii) a time-varying AC voltage and a fixed pressure. For the time-varying pressure input, they tested several small values of the frequency (say, 1–5.5 Hz), and found that the amplitude of the oscillation increases with the frequency of the pressure. For the time-varying AC voltage input, they observed the phenomena of multiple resonance peaks and different vibration modes. These dynamic phenomena of dielectric elastomers have not been explained theoretically. We will compare our theoretical results with their experimental data.

Fig. 12a plots the pressure as a function of the volume for a VHB 4910 membrane in the absence of voltage. The experimental data

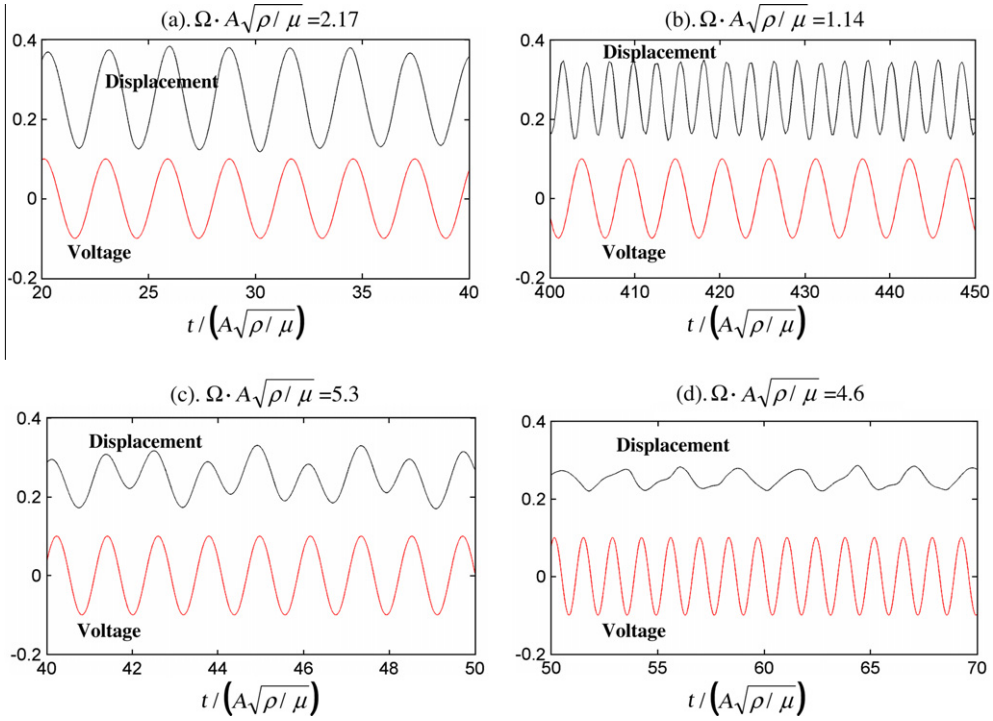

Fig. 11. Harmonic (a,c), superharmonic (b), and subharmonic (d) responses of the membrane when $\frac{pA}{\mu H} = 0.1$, $\frac{\varepsilon \Phi_{dc}^2}{\mu H^2} = 0.01$, and $\frac{\Phi_{ac}}{\Phi_{dc}} = 0.1$.

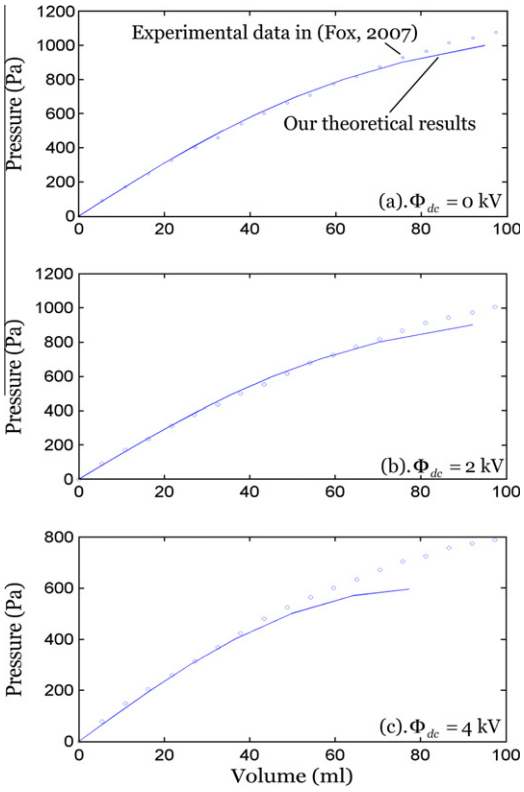

Fig. 12. The pressure is plotted as functions of the volume enclosed by the VHB 4910 membrane at several values of voltage. Our theoretical results are indicated by solid lines, while the experimental data (Fox, 2007) are indicated by circle points.

in Fig. 18 of Fox (2007) match well with our theoretical curve once the shear modulus is set to be 25.1 kPa. The average error is 4%. The difference between the experimental data and theoretical prediction becomes large when the stretch is large, possibly because the neo-Hookean model becomes inaccurate at larger stretches.

When the membrane is subject to two levels of dc voltage, as shown in Fig. 12b and c, the experimental data of Fox (2007) match well with our theoretical curve once the dielectric constant is set to be 4.55, a value reported by Kofod et al. (2003). The difference between the experimental data and theoretical curves becomes large at large stretches. In addition to the possible inaccuracy of the neo-Hookean model, a recent experiment indicates that the dielectric constant may decrease when the elastomer undergoes large deformation (Wissler and Mazza, 2007). In the remainder of this section we will use the shear modulus of 25.1 kPa and dielectric constant 4.55 to calculate theoretical results.

Fox (2007) and Fox and Goulbourne (2008, 2009) analyzed natural frequencies and vibration modes of the VHB 4905 membrane. They tuned the frequency of the AC voltage and recorded the amplitude of the oscillation. For example, when the pressure is 80 Pa, $\Phi_{dc} = 0$, and $\Phi_{ac} = 1.5$ kV, the natural frequencies of out-of-plane oscillation are 70 Hz, 130 Hz and 205 Hz, respectively (Fox, 2007; Fox and Goulbourne, 2009). Based on the method described in Section 4, our theoretical results of natural frequencies are 58.7 Hz, 135.1 Hz, 211.9 Hz for the 1st, 3th, and 5th out-of-plane oscillation, and the average error is about 8%. In analyzing the natural frequencies, we consider the effect of the electrodes, and add the mass of the electrodes to that of the membrane. With a large prestretch (say, $\lambda_0 = 3$), the membrane is very thin and light (even thinner and lighter than the electrodes). For example, in the Fox's experiment, 0.5 ml carbon grease is used, and the mass of the electrodes is about four times that of the membrane itself. The electrodes may significantly decrease natural frequencies of an actuator, especially when the dielectric elastomer is subject to a large prestretch.

Fig. 13 plots superharmonic, harmonic, and subharmonic responses of the VHB 4905 membrane when $p = 80$ pa, $\Phi_{dc} = 0$ kV, $\Phi_{ac} = 1.5$ kV. As stated before, the actual excitation is Φ^2. When $\Phi_{dc} = 0$, the frequency of actual excitation is double that of ac voltage. When the frequency of ac voltage is 29 Hz, as shown in

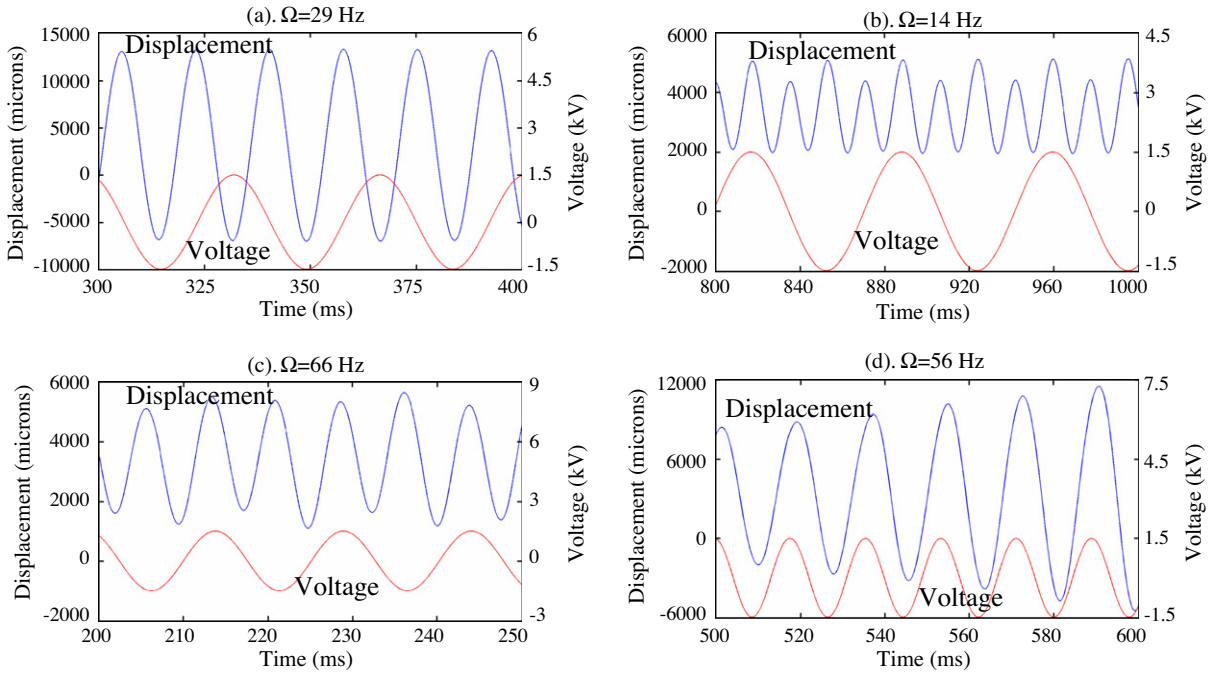

Fig. 13. Harmonic (a,c), superharmonic (b), and subharmonic (d) responses of the VHB 4905 membrane when $p = 80$ pa, $\Phi_{dc} = 0$ kV, $\Phi_{ac} = 1.5$ kV.

Fig. 13a, the frequency of actual excitation is 58 Hz which is close to the first natural frequency (58.7 Hz) as described above. It is seen from Fig. 13a that the frequency of oscillation is about double that of ac voltage (and close to that of actual excitation). This is a harmonic response, similar to the subfigure in Fig. 70 of Fox (2007) where the frequency of ac voltage is 35 Hz, the frequency of actual excitation is 70 Hz, and that of oscillation is about 70 Hz. Fig. 13c is another harmonic response, where the frequency of ac voltage is 66 Hz, the frequency of actual excitation is 132 Hz (which is close to the third natural frequency 135.1 Hz), and the frequency of oscillation is about 132 Hz. This response is similar to another subfigure in Fig. 70 of Fox (2007) where the frequency of ac voltage is 65 Hz. The predicted amplitudes are about ten times those reported in Fox (2007). These large discrepancies are possibly due to that the damping effect is ignored in the current analysis. How dissipation due to viscosity and leakage affects dynamic responses of dielectric elastomer deserves further studies. In addition, our present analysis shows superharmonic and subharmonic responses, but these responses are not reported in the experimental data. When the frequency of ac voltage is 14 Hz, as shown in Fig. 13b, the frequency of actual excitation is 28 Hz (which is close to half of the first natural frequency), the frequency of oscillation is about double that of excitation and four times that of ac voltage. This is a superharmonic response. Fig. 13d shows a subharmonic response. When the frequency of ac voltage is 56 Hz, the frequency of actual excitation is 112 Hz (which is close to double the first natural frequency), the frequency of oscillation is about half of that of excitation, and this is a subharmonic response.

Dubois et al. reported on the active tuning of the fundamental natural frequencies of dielectric elastomer membranes made of PDMS Sylgard 184 and 186 (Dubois et al., 2008). The membranes were prestretched by the fabricated process, and were fixed to a rigid frame. Subject to no pressure, the membranes remained flat, and deformed homogenously. Their natural frequencies were tuned by applying dc voltages through the thickness of the membranes to reduce their internal stress. With the method described in Section 2 and the material, geometry, and loading parameters used in Dubois et al. (2008), we can analyze the natural frequencies of these dielectric elastomer membranes. Fig. 14 compares our theoretical results with Dubois's experimental data. For the 2 mm-diameter Sylgard 186 membrane, the average error of our theoretical results is 7.5%. For the 4 mm-diameter Sylgard 184 membrane, the average error of our results is 2.3%. Because this experiment induces homogeneous deformation in the membrane, the theory and model employed in Dubois et al. (2008) is relative simple. Our theory, however, is also applicable when the membrane undergoes inhomogeneous deformations. In many potential commercial applications (say, Universal Muscle Actuators in AMI), the dielec-

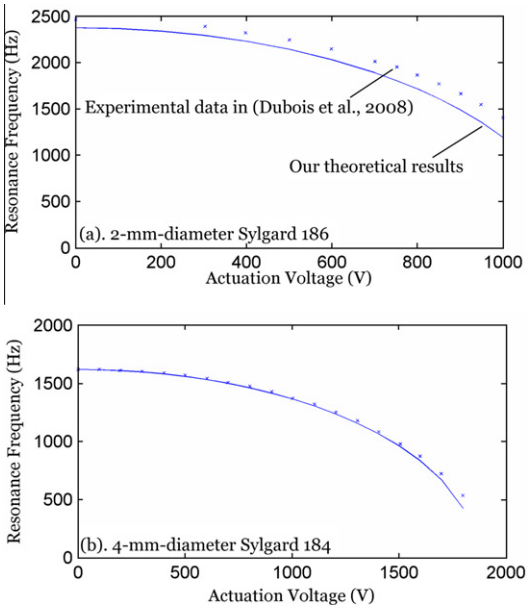

Fig. 14. Tuning the natural frequencies of the Sylgard 184 and 186 membranes. Without pressure, the membrane is flat and in a homogeneous state. Changes in the voltage can tune the natural frequencies of the membranes.

tric elastomers have inhomogeneous deformations (Bonwit et al., 2006; Carpi et al., 2008; He et al., 2009).

8. Concluding remarks

This paper studies nonlinear dynamics of a membrane of a dielectric elastomer. When subject to a static pressure and voltage, the membrane reaches a state of equilibrium. We analyze instability of states of equilibrium, natural frequencies, and vibration modes. When the fundamental natural frequency vanishes, the state of equilibrium becomes unstable. We show that the natural frequencies of dielectric elastomers are tunable by varying the prestretch, pressure, or voltage. When driven by a sinusoidal voltage, the membrane resonates at multiple values of the frequency of excitation, showing different vibration modes. Meanwhile, superharmonic, harmonic and subharmonic responses are found in the present analysis. Our results, e.g. multiple resonance peaks and out-of-plane vibration modes, are consistent with experimental data. We hope that our theoretical predictions, e.g. in-plane vibration modes, superharmonic and subharmonic parametric responses, can be ascertained by future experimental observations.

Acknowledgements

This work is supported by the National Science Foundation through a grant (CMMI-0800161) and by the Kavli Institute at Harvard University. J.Z. acknowledges the support of NSERC postdoctoral fellowship of Canada.

References

Anton, S.R., Sodano, H.A., 2007. A review of power harvesting using piezoelectric materials (2003–2006). Smart Mater. Struct. 16, R1–R21.
Arruda, E.M., Boyce, M., 1993. A three-dimensional constitutive model for the large stretch behavior of rubber elastic materials. J. Mech. Phys. Solids 41, 389–412.
Bonwit, N., Heim, J., Rosenthal, M., Duncheon, C., Beavers, A., 2006. Design of commercial applications of EPAM technology. Proceedings of the SPIE 6168, 39–48.
Bustamante, R., Dorfmann, A., Ogden, R., 2009. Nonlinear electroelastostatics: a variational framework. Z. Angew. Math. Phys. 60, 154–177.
Carpi, F., Rossi, D.D., Kornbluh, R., Pelrine, R., Sommer-Larsen, P., 2008. Dielectric Elastomers as Electromechanical Transducers: Fundamentals, Materials, Devices, Models and Applications of an Emerging Electroactive Polymer Technology. Elsevier, UK.
Chiba, S., Waki, M., Kornbluh, R., Pelrine, R., 2007. Extending applications of dielectric elastomer artificial muscle. In: Proceedings of the SPIE 6524, 652424.
Cottone, F., Vocca, H., Gammaitoni, L., 2009. Nonlinear energy harvesting. Phys. Rev. Lett. 102, 080601.
Den Hartog, J.P., 1985. Mechanical Vibrations. Dover Publications Inc., New York.
De, S.K., Aluru, N.R., 2005. Complex oscillations and chaos in electrostatic microelectromechanical systems under superharmonic excitations. Phys. Rev. Lett. 94, 204101.
Dubois, P., Rosset, S., Niklaus, M., Dadras, M., Shea, H., 2008. Voltage control of the resonance frequency of dielectric electroactive polymer (DEAP) membranes. J. Microelectromech. S. 17, 1072–1081.
Ekinci, K.L., Huang, X.M.H., Roukes, M.L., 2004. Ultrasensitive nanoelectromechanical mass detection. Appl. Phys. Lett. 84, 4469–4471.
Farlow, S.J., 1993. Partial Differential Equations for Scientists and Engineers. Dover Publications, New York.
Fox, J.W., 2007. Electromechanical Characterization of the Static and Dynamic Response of Dielectric Elastomer Membranes, Master thesis, Virginia Polytechnic Institute and State University.
Fox, J.W., Goulbourne, N.C., 2008. On the dynamic electromechanical loading of dielectric elastomer membranes. J. Mech. Phys. Solids 56, 2669–2686.
Fox, J.W., Goulbourne, N.C., 2009. Electric field induced surface transformations and experimental dynamic characteristics of dielectric elastomer membranes. J. Mech. Phys. Solids 57, 1417–1435.
Goncalves, P.B., Soares, R.M., Pamplona, D., 2009. Nonlinear vibrations of a radially stretched circular hyperelastic membrane. J. Sound. Vib. 327, 231–248.
Goulbourne, N.C., Mockensturm, E.M., Frecker, M., 2005. A nonlinear model for dielectric elastomer membranes. ASME J. Appl. Mech. 72, 899–906.
Goulbourne, N.C., Mockensturm, E.M., Frecker, M.I., 2007. Electro-elastomers: large deformation analysis of silicone membranes, Int. J. Solids Struct. 44, 2609–2626.
Ha, S.M., Yuan, W., Pein, Q.B., Pelrine, R., 2006. Interpenetrating polymer networks for high-performance electroelastomer artificial muscles. Adv. Mater. 18, 887–891.
He, T.H., Zhao, X.H., Suo, Z.G., 2009. Dielectric elastomer membranes undergoing inhomogeneous deformation. J. Appl. Phys. 106, 083522.
Heydt, R., Kornbluh, R., Eckerle, J., Pelrine, R., 2006. Sound radiation properties of dielectric elastomer electroactive polymer loudspeakers. In: Proceedings of SPIE 6168, 61681M.
Heydt, R., Pelrine, R., Joseph, J., Eckerle, J., Kornbluh, R., 2000. Acoustical performance of an electrostrictive polymer film loudspeakers. J. Acoust. Soc. Am. 107, 833–839.
Hwang, S.J., Perkins, N.C., 1994. High speed stability of coupled band/wheel systems: theory and experiment. J. Sound. Vib. 169, 459–483.
Jordan, D.W., Smith, P., 1987. Nonlinear Ordinary Differential Equations. Clarendon Press, Oxford.
Kofod, G., Sommer-Larsen, P., Kornbluh, R., Pelrine, R., 2003. Actuation response of polyacrylate dielectric elastomers. J. Intel. Mat. Syst. Str. 14, 787–793.
Mockensturm, E.M., Goulbourne, N.C., 2006. Dynamic response of dielectric elastomers. Int. J. Nonlinear Mech. 41, 388–395.
Nayfeh, A.H., Mook, D.T., 1979. Nonlinear Oscillation. Wiley, New York.
Nguyen, C., 2007. MEMS technology for timing and frequency control. IEEE Trans. Ultrason. Ferr. 54, 251–270.
Pelrine, R., Kornbluh, R., Pei, Q.B., Joseph, J., 2000. High-speed electrically actuated elastomers with strain greater than 100%. Science 287, 836–839.
Suo, Z.G., Zhao, X.H., Greene, W.H., 2008. A nonlinear field theory of deformable dielectrics. J. Mech. Phys. Solids 56, 467–486.
Suo, Z.G., Zhu, J., 2009. Dielectric elastomers of interpenetrating networks. Appl. Phys. Lett. 95, 232909.
Turner, K.L., Miller, S.A., Hartwell, P.G., MacDonald, N.C., Strogatz, S.H., Adams, S.G., 1998. Five parametric resonances in a microelectromechanical system. Nature 396, 149–152.
Wissler, M., Mazza, E., 2005. Modeling and simulation of dielectric elastomer actuators. Smart Mater. Struct. 14, 1396–1402.
Wissler, M., Mazza, E., 2007. Electromechanical coupling in dielectric elastomer actuators. Sensor. Actuat. A-Phys. 138, 384–393.
Zhao, X.H., Hong, W., Suo, Z.G., 2007. Electromechanical coexistent states and hysteresis in dielectric elastomers. Phys. Rev. B 76, 134113.
Zhao, X.H., Suo, Z.G., 2008a. Electrostriction in elastic dielectrics undergoing large deformation. J. Appl. Phys. 104, 123530.
Zhao, X.H., Suo, Z.G., 2008b. Method to analyze programmable deformation of dielectric elastomer layers. Appl. Phys. Lett. 93, 251902.
Zhao, X.H., Suo, Z.G., 2010. Theory of dielectric elastomers capable of giant deformation of actuation. Phys. Rev. Lett. 104, 178302.
Zhu, J., Cai, S.Q., Suo, Z., 2010. Nonlinear oscillation of a dielectric elastomer balloon. Polym. Int. 59, 378–383.
Zhu, J., Ru, C.Q., Mioduchowski, A., 2008. High-order subharmonic parametric resonance of nonlinearly coupled micromechanical oscillators. Eur. Phys. J. B 58, 411–421.